Published online 27 May 2012 *Nucleic Acids Research, 2012, Vol. 40, No. 16* ***8175–8185***
doi:10.1093/nar/gks410

Targeting duplex DNA with chimeric α,β-triplex-forming oligonucleotides

N. A. Kolganova, A. K. Shchyolkina, A. V. Chudinov, A. S. Zasedatelev, V. L. Florentiev and E. N. Timofeev*

Engelhardt Institute of Molecular Biology, Russian Academy of Sciences, Vavilov str. 32, Moscow, 119991, Russia

Received January 23, 2012; Revised April 19, 2012; Accepted April 20, 2012

ABSTRACT

Triplex-directed DNA recognition is strictly limited by polypurine sequences. In an attempt to address this problem with synthetic biology tools, we designed a panel of short chimeric α,β-triplex-forming oligonucleotides (TFOs) and studied their interaction with fluorescently labelled duplex hairpins using various techniques. The hybridization of hairpin with an array of chimeric probes suggests that recognition of double-stranded DNA follows complicated rules combining reversed Hoogsteen and non-canonical homologous hydrogen bonding. In the presence of magnesium ions, chimeric TFOs are able to form highly stable α,β-triplexes, as indicated by native gel-electrophoresis, on-array thermal denaturation and fluorescence-quenching experiments. CD spectra of chimeric triplexes exhibited features typically observed for anti-parallel purine triplexes with a GA or GT third strand. The high potential of chimeric α,β-TFOs in targeting double-stranded DNA was demonstrated in the EcoRI endonuclease protection assay. In this paper, we report, for the first time, the recognition of base pair inversions in a duplex by chimeric TFOs containing α-thymidine and α-deoxyguanosine.

INTRODUCTION

Over 20 years have passed since the principles of triplex-based DNA targeting were experimentally implemented (1,2). In numerous studies, the triplex strategy has proven to have great potential in molecular therapeutics, nanoscience and triplex-mediated gene modification (3–5). However, until now, the main limitation of triplex-directed DNA recognition, the requirement for a polypurine DNA sequence, has not been overcome.

In the last decade, considerable effort has been expended to address this problem with the techniques of synthetic biology (6). Most studies on targeting base pair inversions refer to a pyrimidine triplex motif and exploited either extension of the third strand base to make possible its Hoogsteen-type interactions with a purine in the distant duplex strand or addressing the modified base to a pyrimidine. Both of these techniques were often enhanced by the introduction of fragments responsible for non-specific hydrophobic or ionic interactions (7–9). Recently, the modification repertoire was extended to the attachment of one or more cross-linking groups (10). The method exploring the Hoogsteen interactions with a distant purine seems the most attractive, as it allows rational design of modified nucleotides that would comply with hydrogen bonding rules and triplet geometry. A considerable number of structures designed to interact within the pyrimidine triplex motif with distant purine groups of the inverted base pair have been reported (7,8,11–15). The design of modified bases for the recognition of pyrimidines at inverted sites faces a real challenge, as only one full-featured hydrogen bond can be invoked in this case. A few largely successful examples of such modifications have been described in the literature (16–21).

The purine triplex motif did not draw as much attention as pyrimidine triplexes in targeting base pair inversions. To this end, Sasaki and colleagues have developed a wide panel of bicyclic W-shaped nucleoside analogues (WNA) (22–25). Some of the synthesized base analogues have shown selective stabilization of triplexes with interrupting sites. However, the affinity of WNA analogues appeared to be dependent on the nature of the neighbouring bases (23,25). It is noteworthy that in most triplex studies, the influence of nearest neighbours of the modified base in the TFO on binding specificity has not been considered.

Given the significant progress in the design of synthetic nucleoside analogues capable of binding to inverted sites, the described approaches still fall far short of recognizing random or alternating DNA sequences.

*To whom correspondence should be addressed. Tel: +7 499 1356591; Fax: +7 499 1351405; Email: edward@eimb.ru

© The Author(s) 2012. Published by Oxford University Press.
This is an Open Access article distributed under the terms of the Creative Commons Attribution Non-Commercial License (http://creativecommons.org/licenses/by-nc/3.0), which permits unrestricted non-commercial use, distribution, and reproduction in any medium, provided the original work is properly cited.

Two alternative solutions, which are not mentioned above, invoke Hoogsteen interactions of modified third strand bases with the purines of either duplex strand. In the first method, proposed by Gold and colleagues (26–28), the third strand was built from four non-natural C-glycosides (TRIPsides). Every TRIPside formed two Hoogsteen hydrogen bonds with the purine bases. The TRIPside TFO was shown to target efficiently the DNA duplex and bind a 19-bp DNA duplex by means of four purine–pyrimidine interruptions (28). Another approach was first formulated by Behr and Doronina (29) who proposed an α,β-chimeric TFO strand with different nucleotide anomers facing the purines of two different duplex strands. This idea promised a simple and elegant solution for any sequence combination.

Our efforts in this field were directed to the studies of α-cytidine and α-thymidine as candidates for recognition of AT base pair inversions (30–32). The proposed Hoogsteen bonding of α and β nucleotides with purines (Figure 1) apposes α-nucleotides to the purines of inverted base pairs. Recently, we showed (32) by native polyacrylamide gel electrophoresis that single or five adjacent AT inversions could be recognized by short chimeric TFOs containing αT at 10°C and pH 7.8. Estimation of thermal stability from the slopes of UV melting curves gave T_m values in the range of 10–15°C for 15-mer chimeric triplexes (32). It has been hypothesized that an anomeric switch in the third strand induces a break in the regular structure of the triple helix and that β → α and reverse α → β transitions are not equivalent in their destabilizing effects. Therefore, the stability of the chimeric triplex and precision of duplex targeting is expected to be considerably influenced by the nearest neighbourhood of the inverted base triplet.

In this study, we designed a panel of chimeric α,β-TFOs and assessed the precision of duplex targeting and the stability of formed triplexes by different experimental techniques, including hybridization to an oligonucleotide microarray, native PAGE, thermal denaturation with detection by absorbance and fluorescence and EcoRI restriction endonuclease protection assays. In particular, we analysed hybridization patterns of different fluorescently labelled duplex hairpins with an immobilized set of 15-nt chimeric TFOs. The distribution of fluorescence on the microarray clearly indicates that the efficiency and precision of duplex targeting is dependent on the sequence context. In the course of our hybridization experiments, we realized that the stability of chimeric triplexes has previously been (32) underestimated. Indeed, the high stability of chimeric triplexes was undoubtedly confirmed by thermal denaturation experiments with detection by fluorescence, native PAGE at different temperatures and on-chip thermal denaturation. We also studied the CD spectra of three-stranded complexes with a chimeric GA and GT third strand, which provided proof of triple helix formation. Finally, in ECoRI endonuclease protection assays, we demonstrate targeting of a 23-bp DNA duplex with multiple GC and AT inversions by chimeric α,β-TFOs.

MATERIALS AND METHODS

Oligonucleotide synthesis

DNA oligomers were synthesized using a 3400 DNA/RNA synthesizer (Applied Biosystems). Modifying phosphoramidites and solid supports were purchased from Glen Research and ChemGenes. Aminomodification at the 3′ end was introduced *via* C7 aminolink CPG. Purification of oligodeoxynucleotides was carried out on a Hypersil ODS column (5 mm; 4.6 × 250 mm) using 0.05 M TEAA (pH 7.0) and a linear gradient of MeCN (10–50% and 30 min for DMTr protected oligodeoxynucleotides and 0–25% and 30 min for fully deblocked oligodeoxynucleotides). The flow rate was 1 ml/min. Removal of the 5′-*O*-DMTr group was achieved by treatment with 2% aqueous TFA for 1 min followed by Et_3N neutralization and precipitation with 2% $LiClO_4$ in acetone. Fluorescent labelling of oligonucleotides with the Cy3 dye was carried out as previously described (33). Oligonucleotide composition was confirmed by MALDI mass spectrometry using a Bruker Reflex IV mass spectrometer with hydroxypicolinic acid or 2-amino-5-nitropyridine as a matrix.

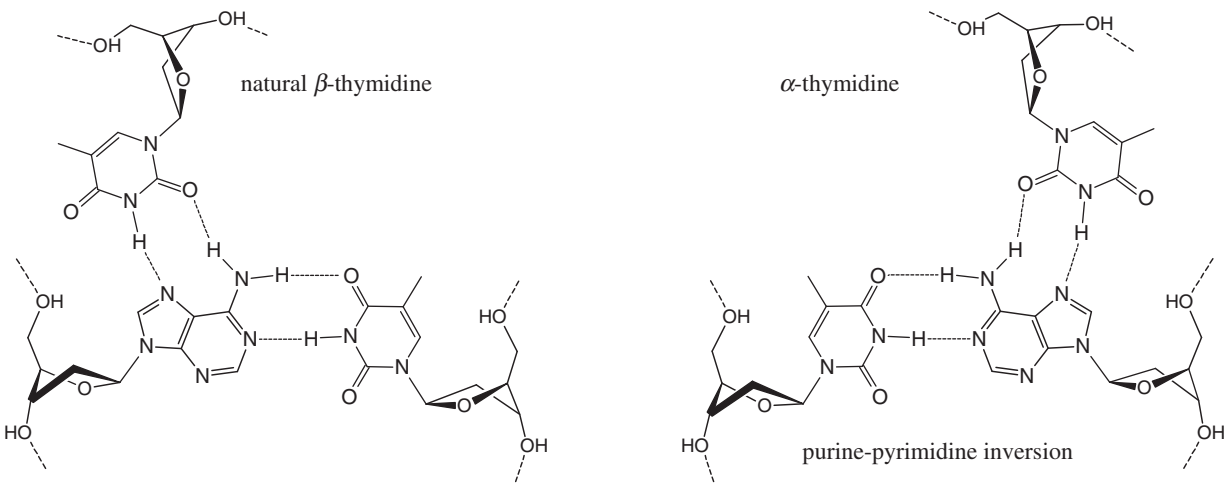

Figure 1. Natural TAT and non-natural (αT)TA triplets.

Microarray manufacturing and hybridization

The array consisted of twelve 150 μm hydrogel pads of hemispherical shape spotted on a hydrophobic glass slide by a pin robot QArray (Molecular Devices). Oligonucleotides were covalently immobilized in the acrylic gel by their 3′ amino groups. Uniform distribution of probes in the gel pads was achieved by simultaneous photo-induced gel polymerization and oligomer immobilization. The final concentration of bound probes in the hydrogel pads was 0.25 mM.

Hybridization of duplex hairpins with chimeric microarrays was carried out in a 100 mM Tris–Borate (pH 7.8) and 30 mM $MgCl_2$ solution containing the labelled targets at a concentration of 1 μM. Hybridization images were taken in real time using an automated custom-made fluorescent research microscope (Biochip-EIMB) equipped with a SenSys CCD camera (Roper Scientific) and a Peltier thermoelectric module (Melcor Corporation). Normalized fluorescent signals (F_{norm}) were calculated by the formula: $F_{norm} = (F - B)/B$, where F is the fluorescent signal from the gel pad and B is the fluorescence of the background around the same gel pad. In the array melting experiments, the temperature was raised at varying rate: 1°C/h (5–10°C), 3°C/h (10–20°C), 6°C/h (20–30°C) and 12°C/h (30–50°C).

UV thermal denaturation

Absorbance versus temperature profiles were obtained with a Shimadzu UV160A spectrophotometer equipped with a water-jacketed cell holder. Dry nitrogen gas was flushed through the cuvette to prevent condensation of water at low temperatures. Melting experiments were measured at 260 nm and with an oligonucleotide concentration of 1 μM in 100 mM Tris–Borate (pH 7.8) and 30 mM $MgCl_2$. The solutions were heated at a rate 0.2°C/min. Melting points were determined from derivative plots of the melting curves.

Native polyacrylamide gel electrophoresis

Polyacrylamide gel electrophoresis assays were performed at varying temperatures under native conditions using a 20% (19:1) acrylamide matrix and a solution of 100 mM Tris–Borate (pH 7.8) and 30 mM $MgCl_2$ as the running buffer. The vertical electrophoresis unit was equipped with a chiller-cooled water jacket. Oligonucleotides were dissolved at a concentration of 10 μM in 10 μl of the above-mentioned buffer in D_2O. Samples were heated to 100°C and cooled slowly to 25°C before loading onto the gel. The gels were run at a constant voltage (7 V/cm).

FRET-mediated quenching in the Cy3-BHQ2 pair

The fluorescence versus temperature profile for the Cy3-BHQ2 quenched triplex **a3–h3** was measured at 568 nm with a Cary Eclipse fluorescent spectrophotometer (Agilent Technologies) equipped with a Peltier cooled cell holder. The excitation wavelength was set to 554 nm. The concentration of the duplex hairpin **h3** was 10 μM in a solution of 100 mM Tris–Borate (pH 7.8) and 30 mM $MgCl_2$. The temperature was raised at a rate 0.5°C/min.

CD spectroscopy

Circular dichroism measurements were carried out with a Jasco-715 CD spectrometer equipped with a Peltier temperature controller. The spectra were obtained at a bandwidth of 1 nm and a spectral resolution of 0.2 nm; three scans were performed.

EcoRI cleavage protection assay

The inhibition of EcoRI duplex cleavage by chimeric TFOs was performed by incubation of labelled DNA duplexes in restriction buffer containing 30 mM $MgCl_2$ for 1 h at 25°C with 30 units of EcoRI (SibEnzyme) in the presence of a 20-fold excess of chimeric TFOs. The concentration of the DNA duplex was 10 μM in a reaction volume of 20 μl. Electrophoresis was carried out with a 20% polyacrylamide gel in 7 M urea and 0.1 M TBE at 25°C.

RESULTS AND DISCUSSION

Hybridization of duplex hairpins with an array of immobilized TFOs

The comparative hybridization of 12 short modified and unmodified oligonucleotides with six duplex hairpin targets was performed in a microarray format. Sequence analysis by hybridization with an oligonucleotide microarray has become a standard procedure in molecular biology. However, the potential of this technique in the analysis of non-canonical DNA structures is still not established. We applied this approach to the screening of interactions between modified TFOs and double-stranded DNA. Chimeric probes were immobilized in arrayed hydrogel elements (34). The topology of the microarray is presented in Figure 2. The targeting α,β oligonucleotides were derived from two parent TFOs with a GA and GT motif, specifically, GAGGGAGAGGAAAAA and GTGG GTGTGGTTTTT. Sequence variations of modified oligonucleotides on the array addressed different issues of triplex formation: the influence of neighbouring nucleotides at sites of base pair inversions, the discrimination of mismatches and the type of TFO probe (GA versus GT), as summarized in Table 1.

The most intriguing observation was the relative high stability of α,β-triplexes in 0.1 M TBE buffer in the presence of magnesium ions. We were able to monitor bright hybridization signals at 25°C from chimeric triplexes **a3–h3** and **a4–h4**, as shown in Figure 2c and d. Moreover, the normalized fluorescence from the chimeric triplex **a3–h3** exceeded the signal from the unmodified triplex **c1–h5** upon hybridization of hairpin **h5** with the microarray. Both the efficiency of hairpin hybridization and the accuracy of duplex targeting by immobilized chimeras appeared to be substantially dependent on the sequence context. Hybridization to the microarray of hairpins **h1–h4** showed their strong preference for probes **a3** and **a4**, as demonstrated by Figure 2a–d. Unexpectedly, probes **a1** and **a2** displayed

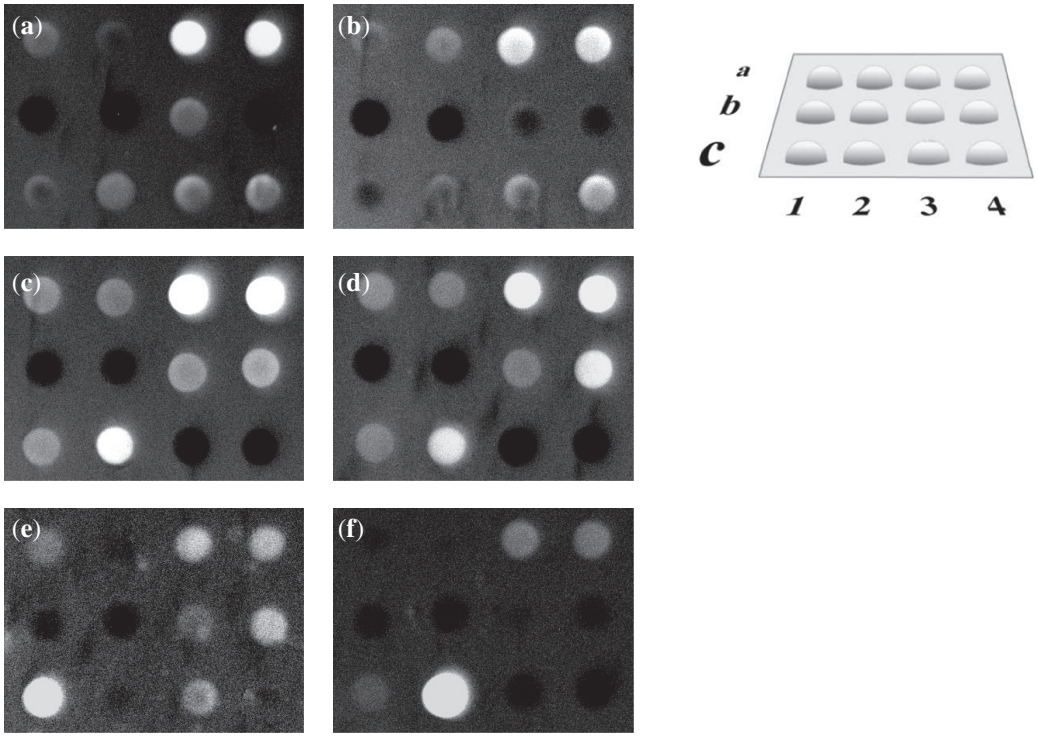

Figure 2. Hybridization of labelled hairpins to the chimeric microarray at 25°C in 100 mM TBE (pH 7.8) and 30 mM $MgCl_2$. (**a**) **h1**; (**b**) **h2**; (**c**) **h3**; (**d**) **h4**; (**e**) **h5**; (**f**) **h6**. Layout of the chimeric microarray (on the right).

Table 1. Chimeric array probes and their expected perfect hairpin targets

Probe	Sequence	Assigned target hairpin sequence	Comments
a1	GAGGGAGAGGA$\underline{T}$AAA	AAATAGGAGAGGGAG-L-CTCCCTCTCCTATTT (**h1**)	Neighbour base variations
a2	GAGGGAGAGGA$\underline{T}$GAA	AAGTAGGAGAGGGAG-L-CTCCCTCTCCTACTT (**h2**)	Neighbour base variations
a3	GAGGGAGAGGG$\underline{T}$AAA	AAATGGGAGAGGGAG-L-CTCCCTCTCCCATTT (**h3**)	Neighbour base variations
a4	GAGGGAGAGGG$\underline{T}$GAA	AAGTGGGAGAGGGAG-L-CTCCCTCTCCCACTT (**h4**)	Neighbour base variations
b1	GAGGG$\underline{T}$GAGGA$\underline{A}$AAA	None	Mismatch
b2	GAGGG$\underline{A}$G$\underline{T}$GGAAAAA	None	Mismatch
b3	GAGGGAG$\underline{A}$GG$\underline{T}$AAAA	None	Mismatch
b4	G$\underline{T}$GGGAGAGG$\underline{A}$AAAA	None	Mismatch
c1	G$\underline{A}$GGGAGAGGAAAAA	AAAAAGGAGAGGGAG-L-CTCCCTCTCCTTTTT (**h5**)	Unmodified GA motif
c2	GAGGGAGAGGAGAAA	AAAGAGGAGAGGGAG-L-CTCCCTCTCCTCTTT (**h6**)	Unmodified GA motif
c3	GTGGGTGTGGTTTTT	AAAAAGGAGAGGGAG-L-CTCCCTCTCCTTTTT (**h5**)	Unmodified GT motif
c4	GTGGGTGTGGT$\underline{T}$TTT	AAATAGGAGAGGGAG-L-CTCCCTCTCCTATTT (**h1**)	Single *a*T GT motif

L = hexaethyleneglycol loop; α-anomers are underlined.

only weak fluorescence upon hybridization with either perfect or mismatched duplex targets. As seen in Table 1, the hairpin targets **h1**–**h4** differed from each other by the neighbouring nucleotides around the inverted base pair. The high-affinity chimeras **a3** and **a4** contained guanine neighbouring αT at the 5′ end of the modified nucleotide. Such an alignment of guanine at the 5′ end of the modification may be required for efficient stacking favouring chimeric triplex formation with a GA third strand. Stacking interruption or a 'stack hole' arising from the α to β transition in the third strand has to be filled to stabilize the triplex structure. Most likely, guanine, rather than adenine, assumes this role. The observed hybridization pattern argues for the dominant role of stacking over hydrogen bonding in recognition. Indeed, the preferred binding of hairpins **h1** and **h2** to the mismatched probes **a3** and **a4**, rather than to the assigned perfect probes **a1** or **a2**, requires formation of mismatched GAT triplets (G targets A). The structurally similar base triplet GTA has been previously described for the pyrimidine triplex motif (35).

Array rows **b1**–**b4** contained chimeras presumably forming mismatched three-stranded complexes when binding with hairpins **h1**–**h4**. The number of supposed mismatched triplets varied from 2 to 4. The mismatched TFO chimeras **b1** and **b2** did not bind either of the duplex targets **h1**–**h4**. Conversely, probes **b3** and **b4** showed noticeable binding to targets **h1**, **h3** and **h4**. The efficiency of their hybridization was comparable to that of probes **a1**

and **a2**, as shown in Figure 2a, c and d. The formation of mismatched chimeric triplexes requires quite unusual base triplets: AGC (A targets G), GAT, ATA, (αT)AT and (αT)GC (Figure 3). Of these base triads, only ATA has been previously examined in regard to its energetics and geometry (36,37). Although most of these base triplets have never been mentioned in the literature, their proposed hydrogen bonding patterns are notably similar to those commonly assumed for three-stranded homologous R-DNA (36,38–40). Such an exotic binding mode combining reversed Hoogsteen and homologous types likely originates from non-isomorphism of chimeric triplexes. The non-isomorphic nature of purine GA/GT triplexes is well-known (41,42). Anomeric transitions in chimeric triplexes require the displacement of the third strand residues, as well. Displacement of the α-nucleotide residue, while targeting purines at the inverted site, may influence the position of neighbouring bases. In turn, depending on the sequence context, this destabilizes the triple helix or makes the formation of mismatches more preferable, thereby preserving stacking at the price of changing the hydrogen bonding mode.

The chimeric oligonucleotide **c4** with a GT sequence motif was designed to bind target **h1**. Hybridization of this probe produced a relatively weak signal (Figure 2a). Nevertheless, the signal was higher than that observed for the perfect probe **a1**. The unmodified GT probe **c3** produced the mismatched complex **c3**–**h1** with a fluorescent intensity at the same level as **c4**–**h1**. Hybridization of hairpin **h2** to the array induced the formation of the relatively stable mismatch **c4**–**h2** with a fluorescent intensity comparable to that of complexes **a3**–**h2** and **a4**–**h2** (Figure 2b). Stabilization of the triplex **c4**–**h2** is believed to be promoted by the homologous type triplet

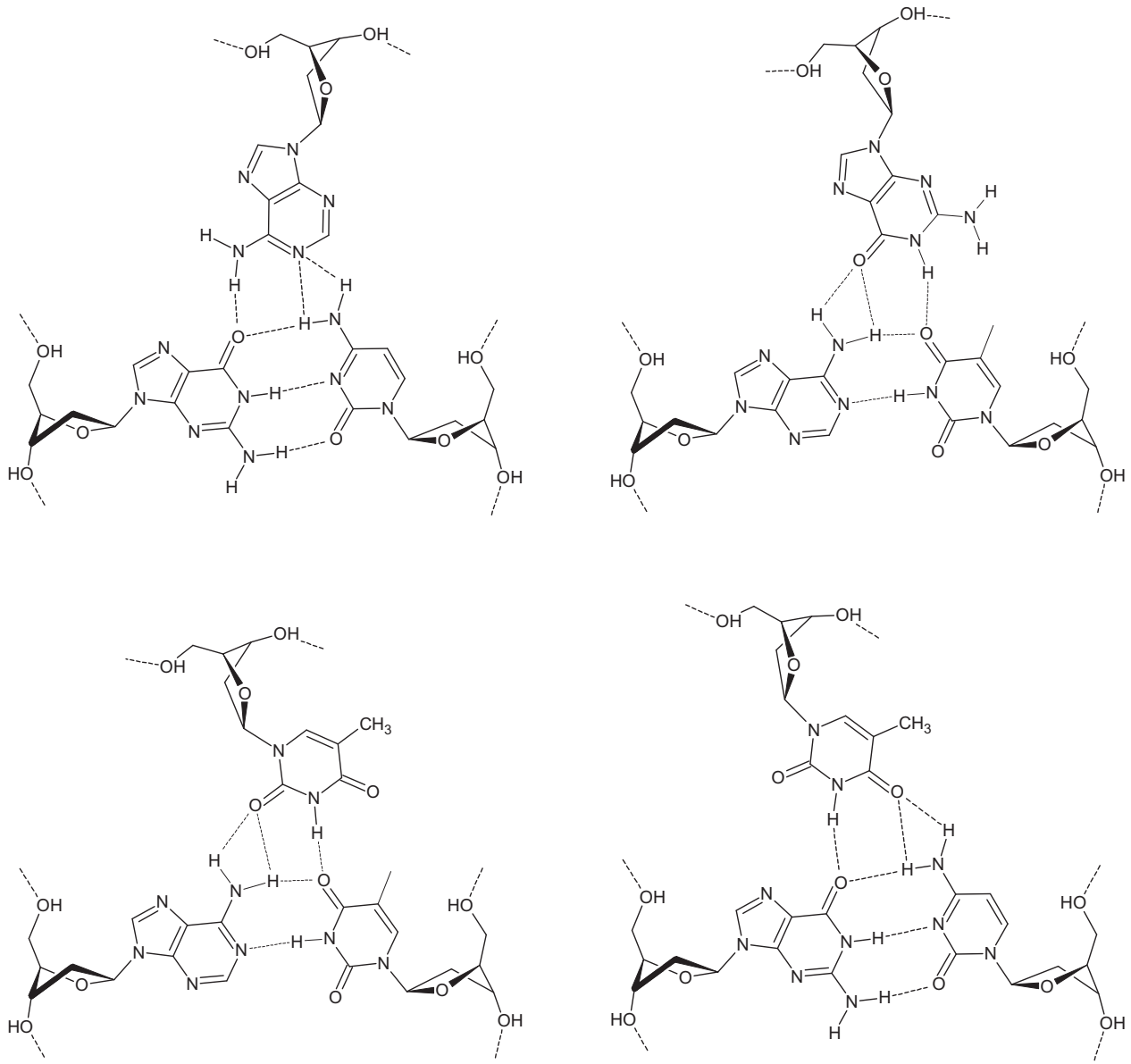

Figure 3. Unusual base triplets: AGC (A targets G), GAT, (αT)AT and (αT)GC.

TGC (T targets G) in the 3′ neighbourhood of the α-nucleotide. The unmodified probe **c3** showed only weak fluorescence upon hybridization with its target duplex **h5** (Figure 2e). The hybridization signal was significantly lower as compared with the unmodified complex **c1**–**h5** with a GA sequence context. The decreased affinity of the GT probes appears to be quite predictable, taking into account the indications in the literature of the lower stability of purine GT triplexes (43–45). As expected, hybridization of hairpin **h6** (Figure 2f) produced a high level of fluorescence from the unmodified perfect probe **c2** along with notably weak signals from mismatched probes **a3**, **a4** and **c1**.

Hybridization behaviour of the labelled hairpins **h1**–**h4** was verified by non-denaturing electrophoresis in polyacrylamide gels (Supplementary Tables S1 and S2). The distribution of the bands in the gel is in good agreement with the hybridization patterns of the duplexes **h3** and **h4** upon binding with probes **a1–a4** on the array. However, interactions of probes **a1**–**a4** with hairpins **h1** and **h2** and probes **b1**–**b4** with hairpins **h2**, **h3** and **h4** did not show the same pattern between the two techniques. The observed variations most likely originate from different conditions of triplex formation in these two methods. Binding of hairpin **h3** with chimeric probes **a1**–**a4** and **b1–b4** followed by a gel-shift assay is shown in Figure 4.

The hybridization data strongly suggest that recognition of double-stranded DNA by chimeric TFOs follows more complicated rules than the Hoogsteen pairing scheme alone. The recognition apparently involves non-canonical base triplets, as required by optimal stacking in a non-isomorphic helical structure.

Thermal stability of chimeric α,β-triplexes

Efficient targeting of selected double-stranded hairpins by microarray-bound chimeras at 25°C undoubtedly indicates a relatively high stability of α,β-triplexes. As shown in Figure 2, probes **a3** and **a4** exhibited highly efficient binding with targets **h1**–**h4**. This observation does not support our previous data on the stability of chimeric α,β-triplexes with a similar sequence context (32). Previously, we estimated the thermal stability of chimeric triplexes in UV denaturation experiments. It has been shown that melting profiles of modified triplexes from three separate strands had low-temperature transitions in the range of 10–15°C. In this study, we used a triplex model with a similar nucleotide sequence and consisting of a duplex hairpin and a separate third strand. This model was expected to have similar UV-melting triplex behaviour. To verify this model, we studied UV denaturation of chimeric triplexes **a1–h1**, **a3–h3** and **c4–h1** in 0.1 M Tris–borate and 30 mM $MgCl_2$ (Supplementary Figure S1). Indeed, the AG triplex **a1–h1** has the same type of melting profile as we observed earlier. However, the chimeric triplex **c4–h1** with a GT third strand and the AG triplex **a3–h3** did not show a low-temperature transition. As mentioned above, complexes **a1**–**h1** and **c4**–**h1** yielded relatively poor fluorescent signals upon hybridization of the labelled target **h1** with the chimeric probe array at 25°C. Thus, low stability of these two complexes could be a good explanation for the observed UV melting profiles. However, the lack of the low-temperature transition for the stable triplex **a3**–**h3** may originate from completely different reasons. Either the triplex-to-duplex transition is not accompanied by an increase in UV absorbance at 260 nm, or triplex melting is monophasic. It should be noted that triplex **a3**–**h3** and duplex hairpin **h3** do not differ from each other by their T_m values (78.8 and 78.4°C). It has been discussed in the literature that anti-parallel triplexes with the GA or GT third strand may show little or no increase in UV absorbance upon denaturation due to considerable stacking in the free third strand (46). On the other hand, monophasic UV melting profiles of anti-parallel GA triplexes have been previously also reported (47).

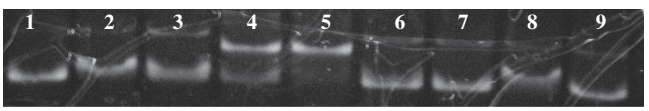

Figure 4. Binding of the hairpin **h3** with chimeric probes **a1–a4** and **b1–b4** at 25°C. (1) Fluorescently labelled hairpin **h3** alone; (2)–(9) labelled hairpin **h3** in the presence of 1.2 equivalents of chimeras **a1–a4** and **b1–b4**.

In order to verify if another wavelength could be used to monitor the dissociation of the third strand, we studied thermal difference spectra (TDS) for complexes **a1–h1**, **a3–h3** and **c4–h1** (48). It was found, however, that over the range 220–320 nm TDS (90 versus 20°C) of triplex and duplex DNA virtually coincide (Supplementary Figure S2). Thus, UV-melting profiles did not provide any support for the results of microarray hybridization or for the idea of a higher triplex stability. In order to obtain a more reliable estimate of triplex stability, we used three other approaches: (i) thermal denaturation of chimeric triplexes on a microarray with fluorescent detection (49), (ii) non-denaturing gel-electrophoresis at different temperatures and (iii) thermal denaturation in solution monitored with the fluorescence of the donor–acceptor pair Cy3-BHQ2.

For microarray melting, we selected the chimeric triplex **a3–h3,** which showed the brightest perfect signal on the array upon hybridization at 25°C. The results of microarray melting experiments for triplexes **a3–h3** and **c1–h5** are presented in Figure 5. Chimeric and unmodified triplexes showed similar stability with temperatures of first derivative peak of 37 and 39°C, respectively. Monitoring of binding affinity to the immobilized probe array as a function of temperature allows direct observation of triplex formation and denaturation. The stability of the triplex **a3–h3** estimated by this method was nearly as high as the stability of the unmodified complex **c1–h5**. We should note, however, that the melting data for the triplex **a3–h3** demonstrates a relatively broad transition, indicating a lower enthalpy of formation of this triplex.

Studies of α,β-triplex formation by native polyacrylamide gel electrophoresis at different temperatures gave us further proof of its high stability. Figure 6 shows native gel electrophoresis of triplexes **a3–h3**, **c1–h5** and **c3–h5** annealed with a 1.5-fold excess of the third strand and run at 30, 40 and 50°C. The duplex hairpin **h3** was taken as a

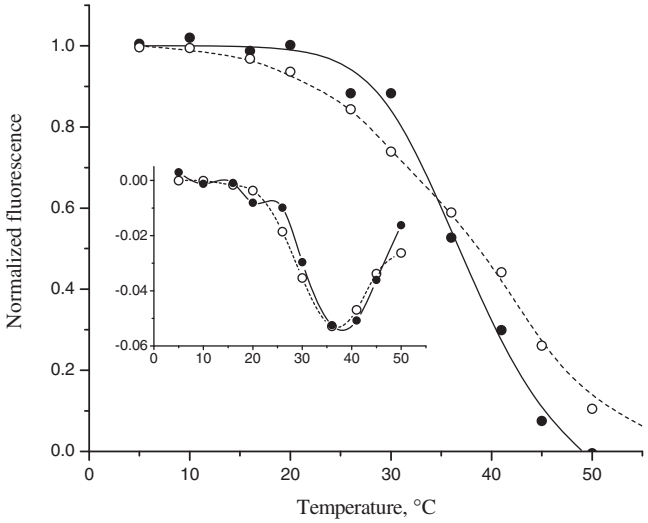

Figure 5. Array melting profiles of chimeric triplexes **a3–h3** (open circles) and **c1–h5** (filled circles) in 0.1 M Tris–borate and 30 mM $MgCl_2$ and a plot of their first derivative.

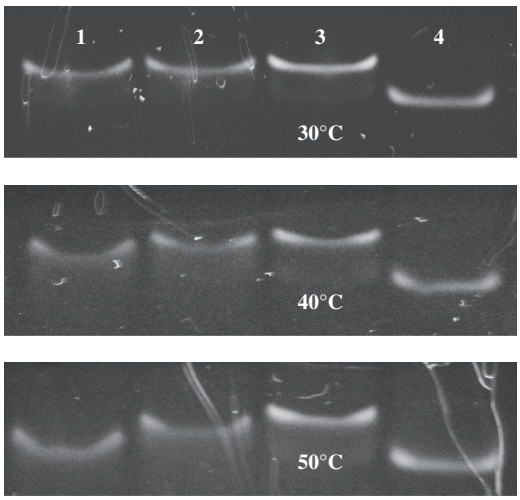

Figure 6. Native gel electrophoresis of triplexes **c3–h5** (1) **c1–h5** (2) and **a3–h3** (3), annealed with a 1.5-fold excess of the third strand and the duplex hairpin **h3** (4) at 30, 40 and 50°C.

control. The chimeric triplex **a3–h3** demonstrated the highest thermal stability with an almost intact low-mobility band at 50°C. The unmodified triplex **c3–h5** with a GT third strand was the least stable and completely dissociated at 50°C. The stability of the natural triplex **c1–h5** was intermediate between complexes **a3–h3** and **c3–h5**. When monitoring triplex bands in the gel-shift experiments at elevated temperatures, we noticed an interesting phenomenon. Instead of being separated into two different species, triplex and duplex DNA, low stability samples (**c1**–**h5** and **c3**–**h5**) showed only one band with an intermediate electrophoretic mobility. A similar co-migration effect for short DNA triplexes has been reported earlier and described by 'cyclic capture and dissociation' model (50). Minor shift of the duplex bands in lanes 2 and 8 in Figure 4 presumably has the same origin.

The duplex hairpins that we used in this study bear a Cy3 fluorescent label at their 3′ end. This allowed us to design a simple model for monitoring thermal denaturation of chimeric triplexes by FRET-mediated quenching in the pair Cy3-BHQ2. The structure of the quenched chimeric triplex **a3–h3** is presented in Figure 7. The localization of the quencher at the 3′ end of the third strand brings it into close proximity to the Cy3 dye upon triplex formation. Dissociation of the third strand would induce an increase in fluorescence intensity. However, at a 1:1 ratio of hairpin to third strand, we were unable to detect a triplex to duplex transition in the range of 15–90°C. In order to minimize the amount of unbound hairpin, we used a 3-fold excess of the third strand **a3**–BHQ2. The fluorescence melting plot of the chimeric triplex **a3–h3** is shown in Figure 7A, curve 1. The steep slope of the curve reflects the temperature dependence of Cy3 dye fluorescence emission. Normalization of the data points to the descending curve of the unquenched hairpin **h3** (curve *2*) resulted in the classical melting profile shown in Figure 7B. The single broad transition of this profile with a melting point of ~65°C gives evidence of monophasic dissociation of the modified triplex. This conclusion is quite consistent with the results of native polyacrylamide gel electrophoresis. The lower thermal stability deduced from microarray melting experiments may originate from unfavourable conditions for hybridization in hydrogel elements. Indeed, unlike single-stranded oligonucleotides, duplex hairpins with increased charge density should present a higher barrier to entry into hydrogel pads saturated with hybridization probes.

CD spectra of chimeric α,β-triplexes

It has been established that DNA triplexes do not have a specific signature in their CD spectra and show considerable variation depending on the sequence (51). Nevertheless, CD spectroscopy has been often used to prove triplex formation (52–56). We studied the CD spectra of the chimeric triplexes **a1–h1** and **c4–h1**. The CD spectrum of the triplex **a1–h1** with a GA sequence context at 0°C (Figure 8A, open circles) characterizes the triplex conformation and is similar to the CD spectra of anti-parallel purine triplexes reported earlier (52). The spectrum is different from the CD spectra of pyrimidine triplexes, which often show a negative peak at 210–220 nm (53). Upon temperature rise to 45°C, the **a1** strand dissociated from the hairpin **h1**, and the sample consisted of duplex hairpins and the single stranded **a1** (Figure 8A, bold circles). The difference CD spectrum (Figure 8A, dashed curve with triangles) indicates the characteristic CD changes associated with AG chimeric triplex formation. The triplex **c4–h1** with a GT third strand exhibited notably different CD spectra, providing more convincing proof of chimeric complex formation. The valley at 266 nm and the reversed temperature dependence of bands in the range of 254–285 nm make the GT triplex easily distinguishable from both duplex DNA and the GA triplex. The CD difference spectrum reflecting formation of the GT type triplex is shown in

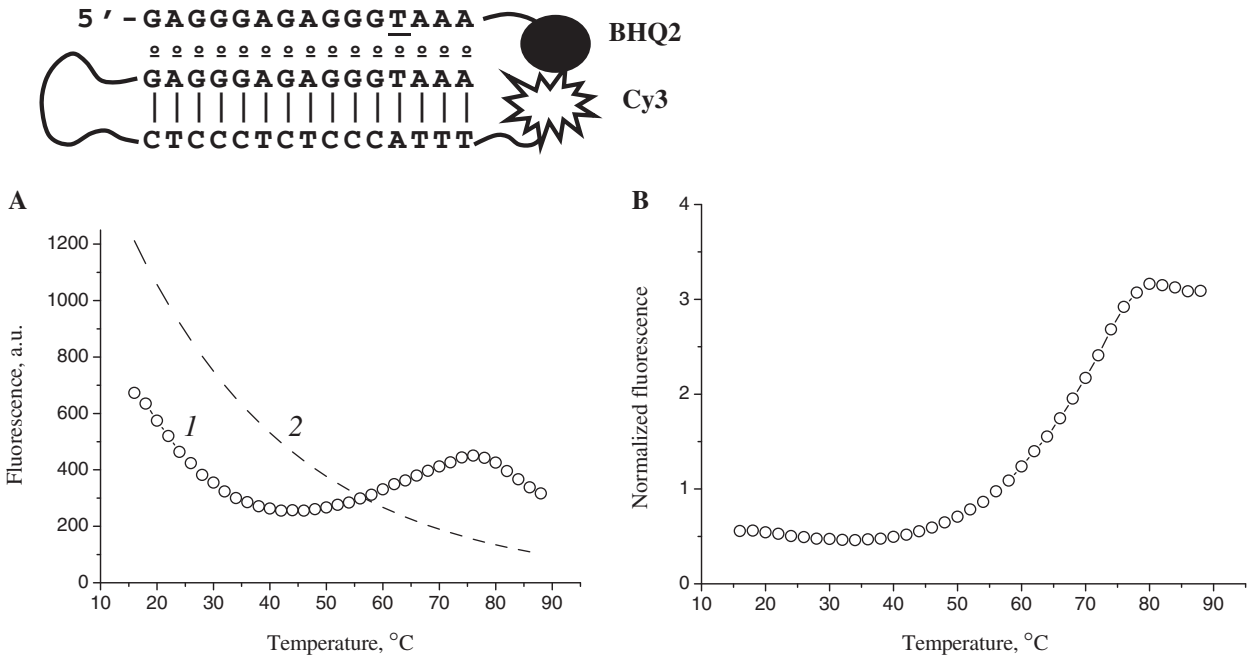

Figure 7. Fluorescence melting plot of the chimeric triplex **a3–h3** (**A**) and normalized melting curve (**B**). 1 triplex **a3–h3**; 2 hairpin **h3**.

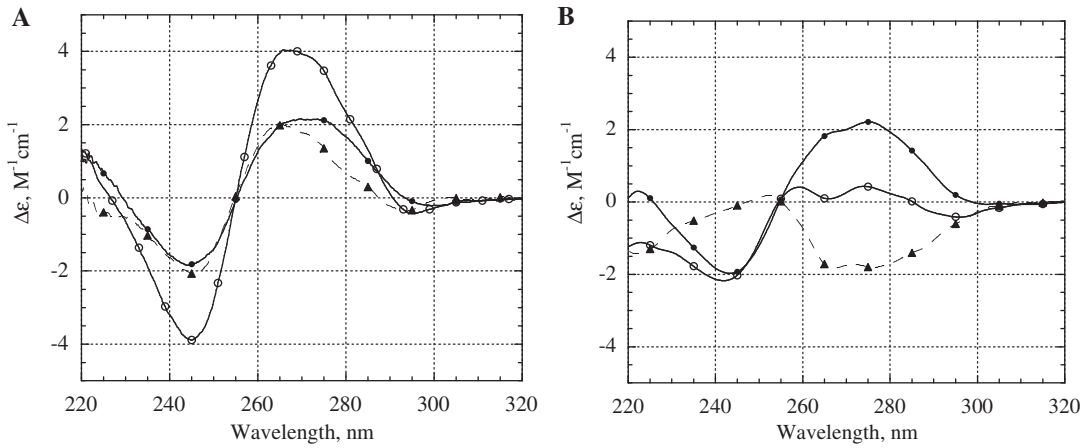

Figure 8. Circular dichroism spectra of triplexes **a1–h1** (**A**) and **c4–h1** (**B**). Temperature was 0°C (open circles) or 45°C (filled circles). Difference CD spectra ($CD^{0°C} - CD^{45°C}$) are shown by the dashed curves with triangles. The concentration of each oligonucleotide was 1.8 μM, and the buffer contained 0.1 M TBE (pH 7.8) and 30 mM $MgCl_2$. Samples were preheated to 80°C and cooled slowly to 0°C before recording CD spectra.

Figure 8B (dashed curve with triangles). Similar changes in CD spectra have been reported in the literature for the unmodified triplex with a GT third strand (55,56).

EcoRI cleavage protection assay

Assuming the higher stability of chimeric triplexes with contiguous inversion stretches, which are closer to the αβ alternate model (57), we designed 23-nt oligonucleotide sequences for an EcoRI restriction assay. The endonuclease EcoRI recognition sequence GAATTC requires at least three consecutive α-nucleotides in the third strand. However, longer uninterrupted α-anomeric tracts are expected to impart higher stability to the chimeric triplex. We constructed three experimental triplex models with TFOs containing a five-base internal modification in the region addressed to the duplex restriction site. Two of these three models contained additional single or four-base inversion sites. Incubation of the Cy3-labelled duplex with EcoRI for 1 h at 25°C in the presence of a 20-fold excess of α,β-TFO inhibited cleavage of double-stranded DNA, as shown in Figure 9. TFO with a single inversion site (model *A*) was the most effective in the restriction assay. The second inversion decreased the ability of TFO to inhibit duplex cleavage by EcoRI. However, TFO containing a second

```
5′-AGAGAGGGAGAGGAATTCCTAGG-Cy3     A
3′-TCTCTCCCTCTCCTTAAGGATCC
3′-AGAGAGGGAGAGGAAttggtAGG

5′-AGAGAGCGAGAGGAATTCCTAGG-Cy3     B
3′-TCTCTCGCTCTCCTTAAGGATCC
3′-AGAGAGgGAGAGGAAttggtAGG

5′-AGTCTCGGAGAGGAATTCCTAGG-Cy3     C
3′-TCAGAGCCTCTCCTTAAGGATCC
3′-AGtgtgGGAGAGGAAttggtAGG
```

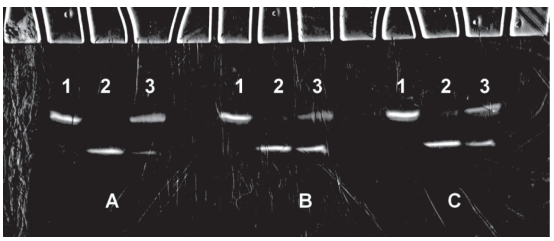

Figure 9. Restriction endonuclease EcoRI cleavage protection by 23-nt chimeric TFOs in models *A*, *B* and *C*. Incubation of labelled DNA duplexes in restriction buffer containing 30 mM $MgCl_2$ for 1 h at 25°C alone (lane 1), with EcoRI (lane 2) and with EcoRI and a 20-fold excess of chimeric TFOs (lane 3). Electrophoresis was done with 20% polyacrylamide gel in 7 M urea and 0.1 M TBE at 25°C. Alpha nucleotides are shown in lower case italics.

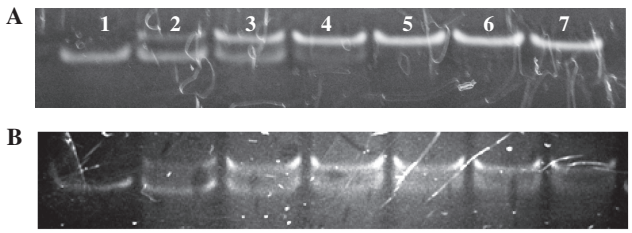

Figure 10. Efficiency of α,β-triplex formation by 23-nt TFOs at 25°C. Triplex *A* (**A**) and mixed triplex $A^{dupl}B^{TFO}$ (**B**). (1) 23-bp duplex; (2–7) 23-bp duplex in the presence of a 0.5-, 1-, 1.5-, 2-, 2.5- and 3-fold excess of the third strand.

four-base α-block (model *C*) provided more efficient cleavage protection compared with a single additional α-nucleotide modification in TFO (model *B*). Thus, inserting longer inversion stretches in chimeric TFOs is more efficient than targeting single base-pair inversions.

The efficiency of α,β-triplex formation by 23-nt TFO (model *A*) at 25°C was monitored by non-denaturing gel-electrophoresis of the fluorescently labelled duplex in the presence of increasing amounts of the third strand (Figure 10A). Virtually complete binding of the duplex with chimeric TFO was observed using a 1.5-fold excess of the third strand. Estimation of the dissociation constant (k_d) gave the value of 1.5 μM (Supplementary Figure S3). To our knowledge, this is the first example of a chimeric DNA triplex with α-thymidine and α-deoxyguanosine in the third strand. Presumable scheme of the hydrogen bonding in (αG)CG triplet is shown in Figure 11.

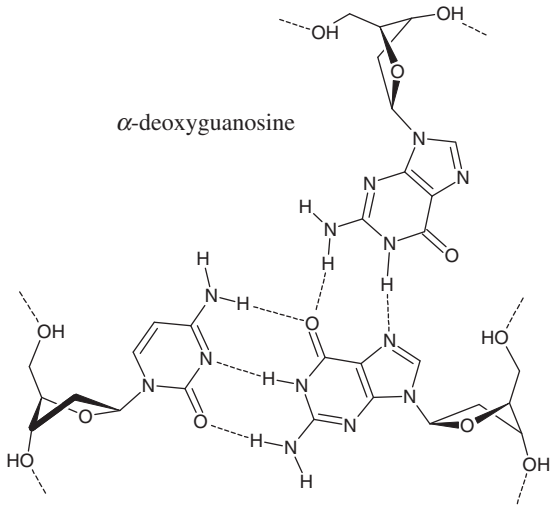

Figure 11. Base triplet (αG)CG.

We have evaluated the precision of duplex targeting with mixed αT–αG chimeric TFO. This was done by addressing chimeric TFOs *B* and *C* to duplex *A*. Mixed three-stranded complex *AB* was formed with decreased efficiency (k_d = 3 μM; Figure 10B). Chimeric TFO *C* was unable to bind duplex *A* up to 20-fold excess of the third strand.

Finally, we studied UV denaturation profiles of the 23-mer chimeric triplexes with contiguous inversion stretches (Supplementary Figure S4). Complexes *A* and *C* showed single transition curves. A biphasic melting curve was obtained for complex *B*. High-temperature transitions were observed at 67.7, 68.6 and 66.8°C for models *A*, *B* and *C*, respectively. Melting temperatures of the underlying duplexes were 68.6, 69.3 and 68.6°C. We tend to consider these data as a support for monophasic transition of the most stable triplex models *A* and *C*.

In conclusion, we demonstrated the high potential of α,β-TFOs in targeting double-stranded DNA. Evidently, the development of a more flexible algorithm in the design of chimeric TFOs that takes non-canonical base triplets into account will extend the range of targeted duplex DNAs.

SUPPLEMENTARY DATA

Supplementary Data are available at NAR Online: Supplementary Tables 1–2 and Supplementary Figures 1–4.

ACKNOWLEDGEMENTS

We thank the staff of the microarray facility, Dr Sergei V. Pan'kov, Eduard Ya. Kreindlin, Olga G. Somova and Olga V. Moiseyeva. We would like to thank Dr Igor P. Smirnov and Dr Andrei A. Stomakhin for their help with the MALDI mass spectrometry of modified oligonucleotides.

FUNDING

The Russian Foundation for Basic Research [08-04-00959, 11-04-01998]; Ministry of Education and Science of the Russian Federation [02.740.11.0845, 16.522.12.2011];

Molecular and Cell Biology program of the Russian Academy of Sciences. Funding for open access charge: Engelhardt Institute of Molecular Biology.

Conflict of interest statement. None declared.

REFERENCES

1. Moser,H.E. and Dervan,P.B. (1987) Sequence-specific cleavage of double helical DNA by triple helix formation. *Science*, **238**, 645–550.
2. Hélène,C. (1991) The anti-gene strategy: control of gene expression by triplex-forming-oligonucleotides. *Anticancer Drug Des.*, **6**, 569–584.
3. Duca,M., Vekhoff,P., Oussedik,K., Halby,L. and Arimondo,P.B. (2008) The triple helix: 50 years later, the outcome. *Nucleic Acids Res.*, **36**, 5123–5138.
4. Tumpane,J., Kumar,R., Lundberg,E.P., Sandin,P., Gale,N., Nandhakumar,I.S., Albinsson,B., Lincoln,P., Wilhelmsson,L.M., Brown,T. *et al.* (2007) Triplex addressability as a basis for functional DNA nanostructures. *Nano Lett.*, **7**, 3832–3839.
5. Sargent,R.G., Kim,S. and Gruenert,D.C. (2011) Oligo/polynucleotide-based gene modification: strategies and therapeutic potential. *Oligonucleotides*, **21**, 55–75.
6. Malnuit,V., Duca,M. and Benhida,R. (2011) Targeting DNA base pair mismatch with artificial nucleobases. Advances and perspectives in triple helix strategy. *Org. Biomol. Chem.*, **9**, 326–336.
7. Rusling,D.A., Powers,V.E., Ranasinghe,R.T., Wang,Y., Osborne,S.D., Brown,T. and Fox,K.R. (2005) Four base recognition by triplex-forming oligonucleotides at physiological pH. *Nucleic Acids Res.*, **33**, 3025–3032.
8. Rusling,D.A., Peng,G., Srinivasan,N., Fox,K.R. and Brown,T. (2009) DNA triplex formation with 5-dimethylaminopropargyl deoxyuridine. *Nucleic Acids Res.*, **37**, 1288–1296.
9. Arya,D.P. (2011) New approaches toward recognition of nucleic acid triple helices. *Acc. Chem. Res.*, **44**, 134–146.
10. Fox,K.R. and Brown,T. (2011) Formation of stable DNA triplexes. *Biochem. Soc. Trans.*, **39**, 629–634.
11. Guianvarc'h,D., Benhida,R., Fourrey,J.L., Maurisse,R. and Sun,J.S. (2001) Incorporation of a novel nucleobase allows stable oligonucleotide-directed triple helix formation at the target sequence containing a purine.pyrimidine interruption. *Chem. Commun.*, **21**, 1814–1815.
12. Guianvarc'h,D., Fourrey,J.L., Maurisse,R., Sun,J.S. and Benhida,R. (2002) Synthesis, incorporation into triplex-forming oligonucleotide, and binding properties of a novel 2′-deoxy-C-nucleoside featuring a 6-(thiazolyl-5)benzimidazole nucleobase. *Org. Lett.*, **4**, 4209–4212.
13. Wang,Y., Rusling,A., Powers,V.E., Lack,O., Osborne,S.D., Fox,K.R. and Brown,T. (2005) Stable recognition of TA interruptions by triplex forming oligonucleotides containing a novel nucleoside. *Biochemistry*, **44**, 5884–5892.
14. Hari,Y., Akabane,M., Hatanaka,Y., Nakahara,M. and Obika,S. (2011) A 4-[(3R,4R)-dihydroxypyrrolidino]pyrimidin-2-one nucleobase for a CG base pair in triplex DNA. *Chem. Commun.*, **47**, 4424–4426.
15. Semenyuk,A., Darian,E., Liu,J., Majumdar,A., Cuenoud,B., Miller,P.S., MacKerell,A.D. and Seidman,M.M. (2010) Targeting of an interrupted polypurine:polypyrimidine sequence in mammalian cells by a triplex-forming oligonucleotide containing a novel base analogue. *Biochemistry*, **49**, 7867–7878.
16. Prévot-Halter,I. and Leumann,C.J. (1999) Selective recognition of a C-G base-pair in the parallel DNA triple-helical binding motif. *Bioorg. Med. Chem. Lett.*, **9**, 2657–2660.
17. Chen,D.L. and McLaughlin,L.W. (2000) Use of pK(a) differences to enhance the formation of base triplets involving C-G and G-C base pairs. *J. Org. Chem.*, **65**, 7468–7474.
18. Obika,S., Hari,Y., Sekiguchi,M. and Imanishi,T. (2001) A 2′,4′-Bridged nucleic acid containing 2-pyridone as a nucleobase: efficient recognition of a CG Interruption by triplex formation with a pyrimidine motif. *Angew. Chem. Int. Ed.*, **1**, 2079–2081.
19. Prévot-Halter,I. and Leumann,C.J. (2002) Evaluation of novel third-strand bases for the recognition of a C center dot G base pair in the parallel DNA triple-helical binding motif. *Helv. Chim. Acta*, **85**, 502–515.
20. Ranasinghe,R.T., Rusling,D.A., Powers,V.E., Fox,K.R. and Brown,T. (2005) Recognition of CG inversions in DNA triple helices by methylated 3H-pyrrolo[2,3-d]pyrimidin-2(7H)-one nucleoside analogues. *Chem. Commun.*, 2555–2557.
21. Gerrard,S.R., Edrees,M.M., Bouamaied,I., Fox,K.R. and Brown,T. (2010) CG base pair recognition within DNA triple helices by modified N-methylpyrrolo-dC nucleosides. *Org. Biomol. Chem.*, **8**, 5087–5096.
22. Sasaki,S., Taniguchi,Y., Takahashi,R., Senko,Y., Kodama,K., Nagatsugi,F. and Maeda,M. (2004) Selective formation of stable triplexes including a TA or a CG interrupting site with new bicyclic nucleoside analogues (WNA). *J. Am. Chem. Soc.*, **126**, 516–528.
23. Taniguchi,Y., Nakamura,A., Senko,Y., Kodama,K., Nagatsugi,F. and Sasaki,S. (2005) Expansion of triplex recognition codes by the use of novel bicyclic nucleoside derivatives (WNA). *Nucleosides Nucleotides Nucleic Acids*, **24**, 823–827.
24. Taniguchi,Y., Nakamura,A., Senko,Y., Nagatsugi,F. and Sasaki,S. (2006) Effects of halogenated WNA derivatives on sequence dependency for expansion of recognition sequences in non-natural-type triplexes. *J. Org. Chem.*, **71**, 2115–2122.
25. Taniguchi,Y., Uchida,Y., Takaki,T., Aoki,E. and Sasaki,S. (2009) Recognition of CG interrupting site by W-shaped nucleoside analogs (WNA) having the pyrazole ring in an anti-parallel triplex DNA. *Bioorg. Med. Chem.*, **17**, 6803–6810.
26. Li,J.S., Shikiya,R., Marky,L.A. and Gold,B. (2004) Triple helix forming TRIPside molecules that target mixed purine/pyrimidine DNA sequences. *Biochemistry*, **43**, 1440–1448.
27. Li,J.S. and Gold,B. (2005) Synthesis of C-nucleosides designed to participate in triplex formation with native DNA: specific recognition of an A:T base pair in DNA. *J. Org. Chem.*, **70**, 8764–8771.
28. Li,J.S., Chen,F.X., Shikiya,R., Marky,L.A. and Gold,B. (2005) Molecular recognition via triplex formation of mixed purine/pyrimidine DNA sequences using oligoTRIPs. *J. Am. Chem. Soc.*, **127**, 12657–12665.
29. Doronina,S.O. and Behr,J.P. (1997) Towards a general triple helix mediated DNA recognition scheme. *Chem. Soc. Rev.*, **26**, 63–71.
30. Timofeev,E.N., Borisova,O.F. and Shchyolkina,A.K. (2000) Structural polymorphism of oligo(dC) with mixed α,β-anomeric backbone. *J. Biomol. Struct. Dyn.*, **17**, 655–664.
31. Timofeev,E.N., Kochetkova,S.V. and Florentiev,V.L. (2004) Binding of nonnatural α,β-oligocytidylates with DNA duplexes. *Mol. Biol.*, **38**, 459–463.
32. Timofeev,E.N., Goryaeva,B.V. and Florentiev,V.L. (2006) Recognition of base pair inversions in duplex by chimeric (α,β) triplex-forming oligonucleotides. *J. Biomol. Struct. Dyn.*, **24**, 183–188.
33. Kolganova,N.A., Florentiev,V.L., Chudinov,A.V., Zasedatelev,A.S. and Timofeev,E.N. (2011) Simple and stereoselective preparation of an 4-(aminomethyl)-1,2,3-triazolyl nucleoside phosphoramidite. *Chem. Biodivers.*, **8**, 568–576.
34. Rubina,A.Y., Pan'kov,S.V., Dementieva,E.I., Pen'kov,D.N., Butygin,A.V., Vasiliskov,V.A., Chudinov,A.V., Mikheikin,A.L., Mikhailovich,V.M. and Mirzabekov,A.D. (2004) Hydrogel drop microchips with immobilized DNA: properties and methods for large-scale production. *Anal. Biochem.*, **325**, 92–106.
35. Wang,E., Malek,S. and Feigon,J. (1992) Structure of a GTA triplet in an intramolecular DNA triplex. *Biochemistry*, **31**, 4838–4846.
36. Lewis,J.P. and Sankey,O.F. (1995) Geometry and energetics of DNA basepairs and triplets from first principles quantum molecular relaxations. *Biophys. J.*, **69**, 1068–1076.
37. Shchyolkina,A.K., Kaluzhny,D.N., Arndt-Jovin,D.J., Jovin,T.M. and Zhurkin,V.B. (2006) Recombination R-triplex: H-bonds contribution to stability as revealed with minor base substitutions for adenine. *Nucleic Acids Res.*, **34**, 3239–3245.
38. Zhurkin,V.B., Raghunathan,G., Ulyanov,N.B., Camerini-Otero,R.D. and Jernigan,R.L. (1994) A parallel DNA triplex as a

model for the intermediate in homologous recombination. *J. Mol. Biol.*, **239**, 181–200.
39. Bertucat,G., Lavery,R. and Prevost,C. (1999) A molecular model for RecA-promoted strand exchange via parallel triple-stranded helices. *Biophys. J.*, **77**, 1562–1576.
40. Shchyolkina,A.K., Timofeev,E.N., Borisova,O.F., Il'icheva,I.A., Minyat,E.E., Khomyakova,E.B. and Florentiev,V.L. (1994) The R-form of DNA does exist. *FEBS Lett.*, **339**, 113–118.
41. Keppler,M.D., Neidle,S. and Fox,K.R. (2001) Stabilisation of TG- and AG-containing antiparallel DNA triplexes by triplex-binding ligands. *Nucleic Acids Res.*, **29**, 1935–1942.
42. Thenmalarchelvi,R. and Yathindra,N. (2005) New insights into DNA triplexes: residual twist and radial difference as measures of base triplet non-isomorphism and their implication to sequence-dependent non-uniform DNA triplex. *Nucleic Acids Res.*, **33**, 43–55.
43. Roy,C. (1993) Inhibition of gene transcription by purine rich triplex forming oligodeoxyribonucleotides. *Nucleic Acids Res.*, **21**, 2845–2852.
44. Faucon,B., Mergny,J.-L. and Hélène,C. (1996) Effect of third strand composition on triple helix formation: purine versus pyrimidine oligodeoxynucleotides. *Nucleic Acids Res.*, **24**, 3181–3188.
45. Jaumot,J., Aviña,A., Eritja,R., Tauler,R. and Gargallo,R. (2003) Resolution of parallel and antiparallel oligonucleotide triple helices formation and melting processes by multivariate curve resolution. *J. Biomol. Struct. Dyn.*, **21**, 267–278.
46. Murphy,D., Eritja,R. and Redmond,G. (2004) Monitoring denaturation behaviour and comparative stability of DNA triple helices using oligonucleotide gold nanoparticle conjugates. *Nucleic Acids Res.*, **32**, e65.
47. Okamoto,I., Ito,S., Takashi,O. and Ono,A. (2009) Synthesis and thermal denaturation studies of covalently linked DNA triplexes. *Nucleic Acids Symp. Ser.*, 165–166.
48. Mergny,J.-L., Li,J., Lacroix,L., Armane,S. and Chaires,J.B. (2005) Thermal difference spectra: a specific signature for nucleic acid structures. *Nucleic Acids Res.*, **33**, e138.
49. Timofeev,E. and Mirzabekov,A. (2001) Binding specificity and stability of duplexes formed by modified oligonucleotides with a 4096-hexanucleotide microarray. *Nucleic Acids Res.*, **29**, 2626–2634.
50. Belotserkovskii,B.P. and Johnston,B.H. (1997) A random-walk model for retardation species during gel electrophoresis: implication for gel-shift assays. *Biophys. J.*, **73**, 1288–1298.
51. Kypr,J., Kejnovská,I., Renciuk,D. and Vorlícková,M. (2009) Circular dichroism and conformational polymorphism of DNA. *Nucleic Acids Res.*, **37**, 1713–1725.
52. Grimau,M.G., Aviñó,A., Gargallo,R. and Eritja,R. (2005) Synthesis and triplex-forming properties of cyclic oligonucleotides with (G,A)-antiparallel strands. *Chem Biodivers.*, **2**, 275–285.
53. Aviñó,A., Frieden,M., Morales,J.C., García de la Torre,B., Güimil García,R., Azorín,F., Gelpí,J.L., Orozco,M., González,C. and Eritja,R. (2002) Properties of triple helices formed by parallel-stranded hairpins containing 8-aminopurines. *Nucleic Acids Res.*, **30**, 2609–2619.
54. Raghavan,S.C., Chastain,P., Lee,J.S., Hegde,B.G., Houston,S., Langen,R., Hsieh,C.L., Haworth,I.S. and Lieber,M.R. (2005) Evidence for a triplex DNA conformation at the bcl-2 major breakpoint region of the t(14;18) translocation. *J. Biol. Chem.*, **280**, 22749–22760.
55. Gondeau,C., Maurizot,J.C. and Durand,M. (1998) Circular dichroism and UV melting studies on formation of an intramolecular triplex containing parallel T*A:T and G*G:C triplets: netropsin complexation with the triplex. *Nucleic Acids Res.*, **26**, 4996–5003.
56. He,Y., Scaria,P.V. and Shafer,R.H. (1997) Studies on formation and stability of the d[G(AG)5]* d[G(AG)5]. d[C(TC)5] and d[G(TG)5]* d[G(AG)5]. d[C(TC)5] triple helices. *Biopolymers*, **41**, 431–441.
57. Shinozuka,K., Matsumoto,N., Suzuki,H., Moriguchi,T. and Sawai,H. (2002) Alternate stranded triplex formation of chimeric DNA composed of tandem alpha- and beta-anomeric strands. *Chem. Commun.*, 2712–2713.